

# High chemical affinity increases the robustness of biochemical oscillations

Clara del Junco and Suriyanarayanan Vaikuntanathan

Department of Chemistry and The James Franck Institute, University of Chicago, Chicago, IL, 60637

Biochemical oscillations are ubiquitous in biology and allow organisms to properly time their biological functions. In this paper, we consider minimal Markov state models of non-equilibrium biochemical networks that support oscillations. Using a perturbation theory, we obtain analytical expressions for the coherence and time period of oscillations in the networks. These quantities are expected to depend on the detailed makeup and arrangement of transition rates in the Markov state model. However, our analytical calculations reveal that many of these details - specifically, the location and arrangement of the transition rates - become irrelevant and contribute minimally to the coherence and time period of oscillations in the limit a high chemical affinity drives the system out of equilibrium. This allows the coherence and time period of oscillations to be robustly maintained and tuned in the limit of high affinity. In a few limited settings, our results also confirm the postulated bound on the coherence of biochemical oscillations set by the chemical affinity of the network (Phys. Rev. E 95, 062409). While recent work has established that increasing energy consumption improves the coherence of oscillations, our findings suggest that it plays the additional role of making the coherence and the average period of oscillations robust to changes that can result from the noisy environment of the cell.

Many organisms possess “internal clocks” implemented as a series of chemical reactions that result in periodic oscillations in the concentrations of certain biomolecules over the course of a day (circadian rhythms [1, 2]), a cell cycle [3], or the development of an embryo (somitogenesis [4, 5]), for example. These oscillations are essential to regulate the timing of biological functions[6]. Biochemical oscillations are found in organisms as small as the cyanobacteria *S. elongatus*, whose circadian rhythm can be reproduced in vitro with only 3 proteins: KaiA, B, and C [7]. The accuracy of the clock is important for the proper functioning of the organism; for instance, the circadian rhythm of *S. elongatus* allows it to anticipate changes in daylight and increases the bacteria’s fitness [1, 8]. Yet, each chemical reaction underlying a biochemical oscillator is a stochastic process, which leads to fluctuations in the period of oscillations and affects how accurately it can tell time. In addition to this *inherent* noise, other aspects of the heterogeneous environment inside a cell can increase the uncertainty in the clock’s period [9]. Understanding how biological organisms can robustly maintain the time scales of their clocks in the presence of these fluctuations is hence a central question [10, 11]. We focus on this question in this letter. Our central result shows that in the limit that the oscillations are driven by a high chemical affinity, the number of relevant parameters that control the period and coherence of oscillations in a biochemical network can decrease dramatically. The insensitivity of the coherence and period of oscillations to changes in a large set of parameters in the high affinity limit makes the oscillations robust (and consequently tunable) even in the presence of fluctuations.

The model we use to derive our results is illustrated in Fig. 1. It consists of  $N$  states connected in a ring topology; these states could represent, for instance, the differ-

ent phosphorylation states of a KaiC protein. The system can hop between states with rates  $k_i^\pm$ , which could represent rates of the (de)phosphorylation reactions. Due to the highly exergonic ATP hydrolysis reaction, the rates of phosphorylation are more favorable than rates of dephosphorylation [12]. Mimicking this asymmetry, the rates in our model networks are generically not balanced, creating a non-equilibrium steady state with a net (clockwise) current from state  $i \rightarrow i + 1$  (clockwise) [13]. The chemical driving force responsible for the current can be quantified by defining the chemical affinity of the network,  $\mathcal{A} \equiv \log \prod_{i=1}^N k_i^+ / k_i^-$  [13]. If the system is initialized on a state  $i_0$  in a network with a non zero affinity and a net current, the probability density vector associated with finding the system in one of the  $N$  states on the network will exhibit damped oscillations. The time period of the oscillations reflects the average time taken by the system to traverse the ring and return to the state  $i_0$ . The damping in the oscillations is an unavoidable consequence of the stochastic nature of the transitions. The ratio of the damping time to the oscillation time provides a figure of merit for the coherence of oscillations in the network [14–17].

In principle, the period and coherence of oscillations depend of the details of the rates  $k_i^\pm$  in the network. However, in line with a large body of work that generically connects energy dissipation to accuracy in biophysical processes [18–23], it has recently been suggested that irrespective of these details the affinity plays an important role in determining the coherence of biochemical oscillations [15, 24]. In particular, Barato and Seifert have conjectured an upper bound on the number of coherent oscillations as a function of the number of states and the affinity of the biochemical network [24]. The bound is saturated when the network is uniform; that is, when all of the counterclockwise (CCW) rates in the network are

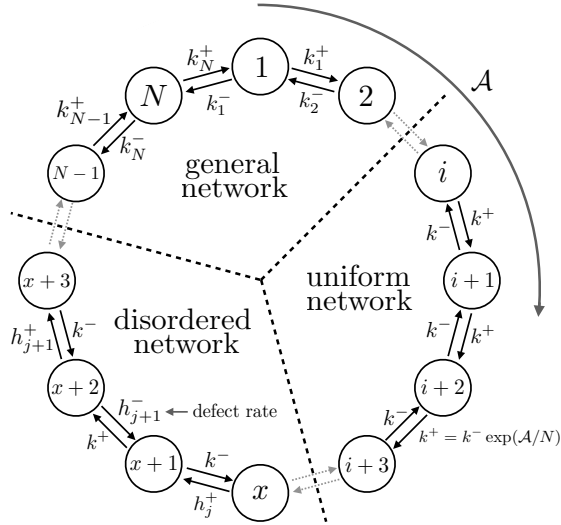


FIG. 1. A network of the kind studied in this paper as a model for a biochemical oscillator. Each node could represent, for instance, a phosphorylation state of a KaiC model, or in a larger system, a vector of concentrations of the different states. The system hops between states with rates  $k_i^\pm$  and is driven out of equilibrium by an affinity  $\mathcal{A}$  so that there is a net clockwise current, resulting in damped oscillations in the probability associated with finding the system in a particular state. In order to analytically probe the dependence of the coherence and time period of oscillations on the rates of the network we begin with a uniform network (for which these quantities are easily computed) and add a fraction of ‘defect rates’  $h_i^\pm$ . We construct a perturbation theory to obtain expression for the coherence and time period of oscillations in such disordered networks.

equal ( $k_i^- = k^- \forall i$ ) and all of the clockwise (CW) rates are equal ( $k_i^+ = k^+ = k^- \exp(\mathcal{A}/N) \forall i$ ).

However, the bound is a weak constraint in many cases [15, 24] and hence the mechanisms, if any, by which a high chemical affinity confers robustness – i.e., allows the timescales of the oscillator to remain constant in the presence of rate fluctuations – remain to be worked out. Our calculations in this letter reveal that the number of relevant parameters that affect these timescales – and hence the coherence of oscillations – decrease dramatically in the limit of high affinity. This renders the timescales robust against a large set of possible changes to the rates in the network.

As in Ref. 24, we use the ratio  $\mathcal{R}$  of the imaginary to real parts of the first non-zero eigenvalue ( $\phi$ ) of the transition rate matrix associated with the Markov state network as a proxy for the coherence of oscillations in the network. We also approximate the period of oscillations by  $T = 2\pi/|\text{Im}[\phi]|$  and the correlation time by  $\tau = -1/\text{Re}[\phi]$ . In practice,  $T$  and  $\tau$  depend on all the eigenvalues of the transition rate matrix. In the Supplementary Material, section I [25], we show that our approximations are sufficient to capture the important features of  $T$  and  $\tau$ .

In order to analytically probe how these properties of biochemical oscillations depend on the rates of the underlying network, we start from a uniform network for which the eigenvalues of the associated transition rate matrix and hence the time scales of oscillation and relaxation are known [26]. We then construct a perturbation theory for changes in the first non-zero eigenvalue,  $\phi$ , when the rates at some fraction of sites are modified from their uniform value – we call these nonuniform rates ‘defects’. As well as constituting a partial proof of the bound in Ref. 24, our main analytical result, summarized in Eqs. 11 – 13, is that the perturbations to  $\phi$  and also to  $\mathcal{R}$ , which in general depend on the values and locations of the defect rates, depend only on the values when the affinity is sufficiently high. This feature means that with a given number of disordered rates,  $\mathcal{R}$  and  $T$  are *predictable* using only the statistics of defect rate magnitudes and *robust* to any changes in the locations of the defect rates and any correlations between them. Numerical results confirm that with high affinity our prediction is accurate for networks with up to 75% defect rates with random values and locations. We also find that high affinity minimizes the change in  $\mathcal{R}$  relative to the uniform network, and significantly decreases the variance of  $\mathcal{R}$  and  $T$  over an ensemble of realizations of the rate disorder. From a biological perspective, our results suggest that in addition to minimizing inherent fluctuations due to stochasticity of the underlying processes [10, 11, 15, 24], a large energy budget makes the number and period of oscillations robust and tunable even in the presence of the additional level of disorder in reaction rates.

**A perturbation theory for  $\mathcal{R}$  and  $T$**  In Ref. 24, Barato and Seifert conjecture that  $\mathcal{R}$  for a fixed  $\mathcal{A}$  and  $N$  is bounded by

$$\mathcal{R} \leq \cot(\pi/N) \tanh[\mathcal{A}/(2N)] \equiv \mathcal{R}_{\text{uniform}} \quad (1)$$

and that the bound is saturated when all of the rates in each direction are equal:  $k_i^+ = k^+ = \exp(\mathcal{A}/N)k^-$  and  $k_i^- = k^-$  for all  $i$ . The transition rate matrix  $\mathbf{W}_0$  for the uniform network is a circulant matrix – a matrix whose  $i$ th row is the top row shifted to the right by  $i$  columns [26]. It has the special property that its eigenvalues are the terms of the discrete Fourier transform of its first row, giving  $\phi^{(0)} = -(k^+ + k^-) + k^+ e^{-2\pi i/N} + k^- e^{2\pi i/N}$  from which  $\mathcal{R}_{\text{uniform}}$  is immediately recovered. We begin from this known result and perturb about the uniform network in order to find how the addition of disorder changes  $\phi$  and therefore  $\mathcal{R}$ .

Rather than directly perturbing  $\mathbf{W}_0$ , we recast the eigenvalue problem in terms of transfer matrices [27]. The transfer matrix formulation is useful for studying properties of systems with high degrees of translational symmetry and rapidly decaying spatial interactions and has been used to study localization in tight binding models [28] and neural networks [29], and dynamic [27] and structural phase transitions [30]. By rearranging each

of the eigenvalue equations  $\mathbf{W}_0 \mathbf{f} = \phi^{(0)} \mathbf{W}_0$  where  $\mathbf{f}$  is the eigenvector corresponding to  $\phi^{(0)}$ , we can recast the eigenvalue equation as:

$$\begin{bmatrix} f_2 \\ f_1 \end{bmatrix} = \mathbf{B}^N \begin{bmatrix} f_2 \\ f_1 \end{bmatrix} \quad (2)$$

where

$$\mathbf{B} = \begin{bmatrix} \frac{\phi^{(0)} + k^- + k^+}{k^+} & -\frac{k^-}{k^+} \\ 1 & 0 \end{bmatrix} \quad (3)$$

$\mathbf{B}$  maps the eigenvector magnitudes  $(f_{i-1}, f_i)$  to  $(f_i, f_{i+1})$  [27].

Since  $\mathbf{B}^N$  must have an eigenvalue of 1 according to Eq. 2, this gives us an alternative to the eigenvalue equation for finding  $\phi^{(0)}$ . Now we consider the effect of changing the rates along  $m$  links of the network from  $k^\pm$  to  $h_j^\pm$  - we refer to  $h_j^\pm$  as a ‘defect rate’. Without loss of generality, we assume that the first defect rates in the network are on either side of state 1. We place the second set of defects around the state located a distance  $L_1 \geq 1$  from state 1, and so forth. The product of transfer matrices in Eq. 2 becomes:

$$\begin{bmatrix} f_2 \\ f_1 \end{bmatrix} = \mathbf{A}_1 \mathbf{B}^{L_1} \dots \mathbf{A}_j \mathbf{B}^{L_j} \dots \mathbf{A}_m \mathbf{B}^{L_m} \begin{bmatrix} f_2 \\ f_1 \end{bmatrix} \quad (4)$$

where the  $A_j$  matrices are the same as  $\mathbf{B}$  but with  $k^\pm$  replaced by  $h_j^\pm$ , and  $\sum_{j=1}^m L_j = N - m$ . In modifying the network in this manner we have changed the eigenvalues of  $\mathbf{W}$ , so that  $\mathbf{B}$  is no longer a function of  $\phi^{(0)}$  but of a new  $\phi$ . We assume that the perturbed value of  $\phi$  has the form:

$$\phi = \phi^{(0)} + C\gamma/N + \mathcal{O}(1/N^2) \equiv \phi^{(0)} + \phi^{(1)} + \mathcal{O}(1/N^2). \quad (5)$$

where  $C$  is a constant that we choose for convenience. Inserting Eq. 5 in to Eq. 3 we obtain  $\mathbf{B} = \mathbf{B}_0 + \mathbf{B}_1$  where  $\mathbf{B}_1 = \{\{C\gamma/(Nk^+), 0\}, \{0, 0\}\}$ . We can now find the eigenvalues  $\beta_i$  of  $\mathbf{B}$  using the usual first-order eigenvalue perturbation expression [27, 31]. We obtain:

$$\beta_1 = \beta_1^{(0)} + \beta_1^{(1)} = e^{-2\pi i/N} (1 + \frac{\gamma}{N}) \approx e^{(-2\pi i + \gamma)/N} \quad (6)$$

$$\beta_2 \approx \frac{k^-}{k^+} e^{(2\pi i + \gamma)/N} = e^{-A/N} e^{(2\pi i + \gamma)/N} < 1 \quad (7)$$

We can then approximate  $\mathbf{B}^{L_j}$  using the first-order eigenvalues and zero-order eigenvectors of  $\mathbf{B}$ :

$$\mathbf{B}^{L_j} = \sum_i \beta_i^{L_j} \mathbf{X}_i \quad (8)$$

where  $\mathbf{X}_i$  is the the outer product of the  $i$ th eigenvector of  $\mathbf{B}$  ( $|i\rangle\langle i|$ ). Plugging this back in to Eq. 4 yields an expression with terms that depends on all of the values of the defect rates ( $h_j^\pm$ ) as well as their spacings ( $L_j$ ) and the order in which they appear. However, since  $\beta_2 \propto$

$e^{-A/N} < 1$ , we can see that if  $e^{-AL_j/N}$  is sufficiently small, all of the terms containing  $\beta_2$  will vanish. In this limit, combining Eq. 4 and 8, we get:

$$\begin{bmatrix} f_2 \\ f_1 \end{bmatrix} = \beta_1^{N-2m} \prod_{j=1}^m \mathbf{Z}_j \begin{bmatrix} f_2 \\ f_1 \end{bmatrix} \quad \mathbf{Z}_j \equiv \mathbf{A}_j \mathbf{X}_1^{(0)} \quad (9)$$

We can now compute the matrix product in Eq. 9 and set its eigenvalue equal to 1 in order to solve for  $\phi$ . In principle, the order of the matrices in the matrix product in Eq. 9 is important and hence the values of  $\phi$  and  $\mathcal{R}$  depend on the order of the defects. However, our calculations are simplified due to a special symmetry in the  $\mathbf{Z}_j$  matrices, which have the form:

$$\begin{bmatrix} c_j a & c_j b \\ a & b \end{bmatrix}, \quad (10)$$

where the specific algebraic expressions for  $c_j$ ,  $a$ , and  $b$  are provided in SM Eq. 29-31 [25]. These matrices have two properties that are relevant here: first, since the two rows of  $\mathbf{Z}_j$  are related by a constant,  $\mathbf{Z}_j$  has a zero eigenvalue. Second, the eigenvalue of the product  $\mathbf{Z}_i \mathbf{Z}_j$  is the product of the eigenvalues of  $\mathbf{Z}_i$  and  $\mathbf{Z}_j$ . Given these two properties, the expression for  $\phi$  is simply determined by the non-trivial eigenvalue of the product of  $\mathbf{Z}_j$  matrices which in turn is simply equal to the product of the non-trivial eigenvalue of the  $\mathbf{Z}_j$  matrices. The order in which the defects are placed, the spacing between them, or any other higher order correlation hence becomes irrelevant as far as  $\phi$  is concerned. Specifically, for a network of size  $N$  with  $m$  defects at any positions we find:

$$\phi = \phi^{(0)} - \frac{C \log \prod_{j=1}^m \chi_j}{(N/m) - 1} = \phi^{(0)} - \frac{C \sum_{j=1}^m \log \chi_j}{(N/m) - 1}. \quad (11)$$

where  $\chi_j$  is given in SM Eq. 32 and 37, along with detailed perturbation theory calculations in SM section II [25]. We emphasize that all of these simplifications are possible only if the affinity is sufficiently high. In particular, the  $X_2$  matrices in Eq. 8 (which do not contribute to  $\phi$  in the high affinity limit for the reasons described above) do not have the same symmetries and result in eigenvalues  $\phi$  that depend on the order and spacing of defect rates. Thus,  $e^{-AL_j/N}$  sets a length scale for correlations between defect rates; in the limit of very high affinity, the effect of even adjacent defect rates can be uncorrelated. We illustrate this in SM section III [25] and in Figs. 3, 4 where we show that when the affinity is small, the location of the defects become important.

Eq. 11 predicts that each defect will contribute an additive term to  $\phi$  in the limit of high affinity. Although the full expression for  $\chi_j$  is cumbersome, the features and limitations of our perturbation theory result are illus-

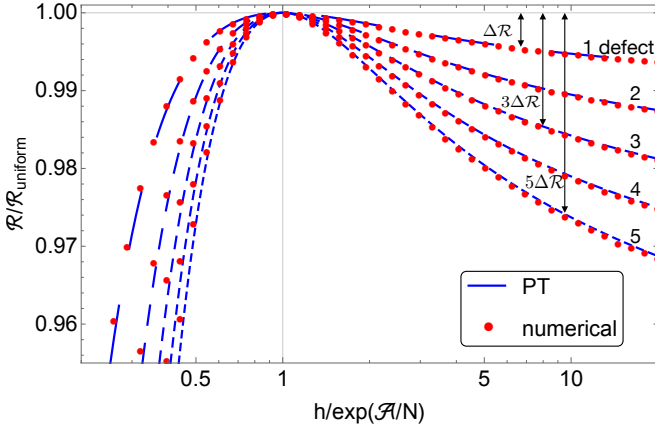


FIG. 2.  $\mathcal{R}$  decreases linearly with each added defect for large  $N$  and  $\mathcal{A}/N$ . Perturbation theory prediction from Eq. 11 and numerical results for  $\mathcal{R}$  as a function of  $(h^+/h^-)/(k^+/k^-) \equiv h/k \equiv h/\exp(\mathcal{A}/N)$ , in a network with  $N = 200$  and  $\mathcal{A} = 500$  with 1 - 5 defect rates. All of the defect rates are the same in these networks. Each numerical data point was generated from a different matrix with the defect spacing randomly chosen from a uniform distribution  $[1, 2N/m]$  where  $m$  is the number of defects, to show that the result is insensitive to the defect spacing in the limit of high affinity.

trated by looking at the large- $N$  expansion of  $C \log(\chi_j)$ :

$$\text{Im}[C \log(\chi_j)] \propto \left(1 + \frac{2}{N}\right) \frac{k^+}{h_j^+} + \mathcal{O}(1/N^2) \quad (12)$$

$$\text{Re}[C \log(\chi_j)] \propto \frac{2\pi^2}{N(k^+ - k^-)} \frac{k^+}{h_j^{+2}} + \mathcal{O}(1/N^2). \quad (13)$$

Our perturbation theory will fail, if  $N$ ,  $\frac{h^+}{k^+}$ , or  $k^+ - k^- \propto \exp(\mathcal{A}/N)$ , or  $N/m$  (inverse fraction of defects), are small. Since the imaginary part of  $\phi^{(1)}$  shows up to order  $1/N$  while the real part appears only to order  $1/N^2$ , provided that  $N$ ,  $\frac{h^+}{k^+}$ , and  $k^+ - k^-$  are sufficiently large,  $\text{Re}[\phi^{(1)}] \ll \text{Im}[\phi^{(1)}]$ . Recalling that the number of oscillations is  $\mathcal{R} = |\text{Im}[\phi]|/|\text{Re}[\phi]|$ , since  $\text{Re}[\phi]$  does not change much compared to  $|\text{Im}[\phi]|$  each defect will also contribute an additive term to  $\mathcal{R}$ , as we show in Fig. 2.

**Randomly distributed defect rates.** To test the limits of this analytical result, we compared it to the result of numerical diagonalization for networks of size  $N = 100$  with 2 – 75% defect rates. In addition, to study the more realistic case that the defect rates are not all known and may change over time or between different instances of the biochemical oscillators (e.g. in different cells), we considered networks with quenched disorder and selected the defect rates randomly from a probability distribution. Our analytical prediction is made by averaging  $\Delta\mathcal{R}_1 = \mathcal{R}_{\text{uniform}} - \mathcal{R}_1$ , where  $\mathcal{R}_1$  is the ratio for a network with a single defect computed from Eq. 11, over 10 000 values of the single defect rate. We then calculate  $\langle\mathcal{R}_m\rangle = \mathcal{R}_{\text{uniform}} - m\langle\Delta\mathcal{R}_1\rangle$ . The numerical results

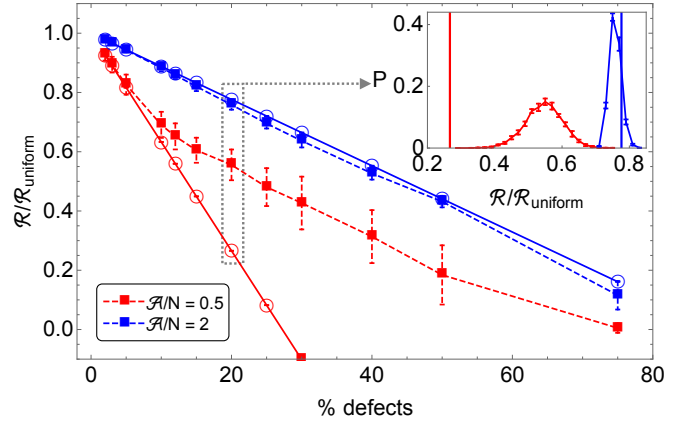


FIG. 3. High affinity increases predictability and decreases variance of  $\mathcal{R}$ . Prediction of  $\mathcal{R}$  for network with  $N = 100$  from perturbation theory (circles/solid lines) and numerical diagonalization (squares/dashed lines). All CCW rates are set to 1. The defect rates were generated by choosing  $h_i^+/\exp(\mathcal{A}/N)$  from a uniform distribution between 1 and 20, which results in a distribution of  $h_i^+/k^+$  values of roughly 1 to 60 once  $k^+$  is adjusted to maintain a constant  $\mathcal{A}$ . At  $\mathcal{A}/N = 2$ , the perturbation theory prediction is accurate with up to 75% defects in the network, and the standard deviation (error bars) of the numerical values is small. At  $\mathcal{A}/N = 0.5$ , the perturbation theory prediction fails for over 5% defects, and the range of possible  $\mathcal{R}$  values is much larger. Inset: Histogram of 10 000 numerical values for a network with 20% defects. The vertical lines are located at the perturbation theory prediction.

were obtained by numerically diagonalizing a sample of 100 transition rate matrices with  $m$  defect rates chosen from the same distribution.

In Fig. 3, we show the importance of a high chemical affinity for controlling the coherence figure of merit  $\mathcal{R}$ . The additive approximation improves with increasing  $\mathcal{A}/N$  for a given distribution of disorder. Fig. 3 shows that our analytical result (based on the one-defect case) can predict  $\langle\mathcal{R}\rangle$  even when up to 75% of the rates in the network have been modified such that  $\langle\mathcal{R}\rangle$  is decreased by 80% from  $\mathcal{R}_{\text{uniform}}$ . Our numerical results also confirm that increasing  $\mathcal{A}$  decreases the spread of  $\mathcal{R}$  values (Fig. 3, inset) because it renders the locations of the defects irrelevant to the value of  $\mathcal{R}$ . In SM Fig. 4 (and accompanying discussion) [25] we show for what distributions of the defect rates the perturbation theory is most valid. From a biophysical perspective, Fig. 3 shows how a high chemical affinity can decrease the number of relevant variables that can affect  $\mathcal{R}$  and hence allow the number of coherent biochemical oscillations to be maintained more robustly. We emphasize that we adjust the  $k^+$  rates as the fraction of defects is changed in order to maintain a constant affinity in Fig. 3. The change in the value of  $\mathcal{R}$  with increasing defect density, even at the constant higher affinity value considered in Fig. 3, shows how the bounds obtained in Ref. [24] can be weak constraints.

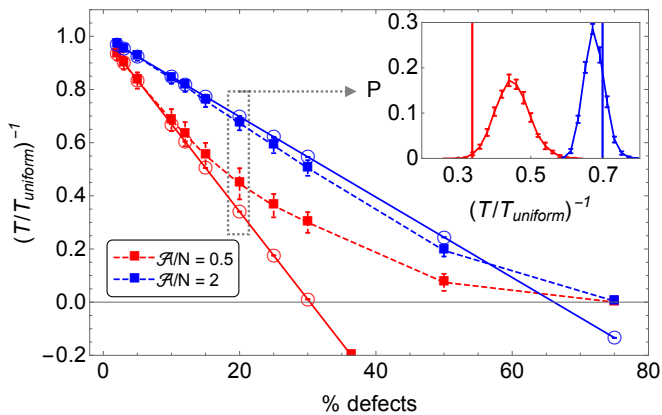


FIG. 4. **High affinity increases predictability and decreases variance of  $T$ .** Prediction of  $(T/T_{\text{uniform}})^{-1}$ , where  $T_{\text{uniform}}$  is the period of oscillations with uniform rates, for a network with  $N = 100$  from perturbation theory (circles/solid lines) and numerical diagonalization (squares/dashed lines). The rates are chosen as in Fig. 3. At  $A/N = 2$ , the perturbation theory prediction is accurate with up to 50% defects in the network, and the standard deviation (error bars) of the numerical values is small. At  $A/N = 0.5$ , the perturbation theory prediction fails around 10% defects, and the range of values is much larger. Inset: Histogram of 10 000 numerical  $(T/T_{\text{uniform}})^{-1}$  values for a network with 20% defects. The vertical lines are located at the perturbation theory prediction.

**Period of oscillations.** While minimizing phase diffusion and thereby maximizing  $\mathcal{R}$  is a priority for a biochemical clock to keep time accurately, it is additionally important that  $T$ , the time period of oscillations, be robust and tunable, for example in order to match with an external signal [8]. In Fig. 4, we show that Eq. 11 can accurately predict  $\langle (T/T_{\text{uniform}})^{-1} \rangle = \langle \text{Im}[\phi] / \text{Im}[\phi^{(0)}] \rangle$  for up to 50% defects and an 80% decrease in  $\langle (T/T_{\text{uniform}})^{-1} \rangle$ . In addition, within our perturbation theory, the conditions for  $\text{Im}[\phi]$  to be linearly proportional to the number of defects are more relaxed than for  $\mathcal{R}$  (SM Fig. 5 [25]). These results suggest that, as for the coherence of oscillations, a high chemical affinity makes the period of oscillations tunable and robust to changes in the rates.

**Discussion and Conclusions.** Biochemical oscillators, which can function as internal clocks, operate in noisy environments that can affect the ability of the clock to tell time accurately; yet somehow these oscillations continue with a well-defined period over long times. Here, we present analytical calculations supported by numerical results that show how a biochemical oscillator modeled as a Markov jump process on a ring of states (Fig. 1) can use high chemical affinity (for instance, in the form of ATP) to robustly maintain and tune its timescales even in the presence of a substantial amount of disorder. While previous work [24] has postulated an upper bound on the number of coherent oscillations such a model can

support in terms of the chemical affinity, the bound can be loose, and does not elucidate the dependence of the number of oscillations on the details of the rates in the network [24]. We close this gap by showing how in the limit of high affinity, the number of relevant variables controlling the coherence and time scales of oscillations dramatically decreases. Specifically, we consider Markov state networks such as those in Fig. 1 and sample a finite fraction of the rates from a probability distribution in order to mimic disorder in biological systems. Our analytical theory reveals that in the limit of high affinity, the period of oscillations and  $\mathcal{R}$  depend only on the statistics of the probability distributions from which the kinetic rates are sampled. Factors such as the distance between the links with disorder or correlations between disorder thus become irrelevant, and the timescales of oscillations are robust to fluctuations in these variables. Our results also constitute a limited proof, within the perturbative regime, of the bound conjectured in Ref. 24. More than that, though, they give insight in to why organisms might evolve to consume more energy in the form of ATP than strictly necessary in a biochemical oscillator [32]: in addition to the previously known functions of suppressing uncertainty in the timescales of the oscillator for a system with uniform rates [15, 24], it also makes  $\mathcal{R}$  and  $T$  more robust to fluctuations in the rates caused by the noisy environment of the cell. In future work, it will be interesting to consider the implications of our results for the entrainment of noisy biochemical oscillators to external signals.

## ACKNOWLEDGEMENTS

CdJ acknowledges the support of the Natural Sciences and Engineering Research Council of Canada (NSERC). CdJ a été financée par le Conseil de recherches en sciences naturelles et en génie du Canada (CRSNG). This work was partially supported by the University of Chicago Materials Research Science and Engineering Center (MRSEC), which is funded by the National Science Foundation under award number DMR-1420709. SV also acknowledge support from the Sloan Fellowship and the University of Chicago.

- 
- [1] C. H. Johnson, C. Zhao, Y. Xu, and T. Mori, *Nat. Rev. Microbiol.* **15**, 232 (2017).
  - [2] S. Panda, J. B. Hogenesch, and S. A. Kay, *Nature* **417**, 329 (2002).
  - [3] J. E. Ferrell, T. Y.-C. Tsai, and Q. Yang, *Cell* **144**, 874 (2011).
  - [4] J. Lewis, *Curr. Biol.* **13**, 1398 (2003).
  - [5] I. Palmeirim, D. Henrique, D. Ish-Horowicz, and O. Pourquié, *Cell* **91**, 639 (1997).

- [6] B. Novák and J. J. Tyson, Nat. Rev. Mol. Cell Biol. **9**, 981 (2008).
- [7] M. Nakajima, K. Imai, H. Ito, T. Nishiwaki, Y. Murayama, H. Iwasaki, T. Oyama, and T. Kondo, Science. **308**, 414 (2005).
- [8] M. A. Woelfle, Y. Ouyang, K. Phanvijhitsiri, and C. H. Johnson, Curr. Biol. **14**, 1481 (2004).
- [9] W. Pittayakanchit, Z. Lu, J. Chew, M. J. Rust, and A. Murugan, Elife **7** (2018), 10.7554/eLife.37624.
- [10] A. C. Barato and U. Seifert, Phys. Rev. Lett. **114**, 158101 (2015).
- [11] T. R. Gingrich, J. M. Horowitz, N. Perunov, and J. L. England, Phys. Rev. Lett. **116**, 120601 (2016).
- [12] M. J. Rust, J. S. Markson, W. S. Lane, D. S. Fisher, and E. K. O'Shea, Science. **318**, 809 (2007).
- [13] U. Seifert, Rep. Prog. Phys. **75**, 126001 (2012).
- [14] H. Qian and M. Qian, Phys. Rev. Lett. **84**, 2271 (2000).
- [15] Y. Cao, H. Wang, Q. Ouyang, and Y. Tu, Nat. Phys. **11**, 772 (2015).
- [16] L. G. Morelli and F. Jülicher, Phys. Rev. Lett. **98**, 228101 (2007).
- [17] B. Nguyen, U. Seifert, and A. C. Barato, J. Chem. Phys. **149**, 045101 (2018).
- [18] J. J. Hopfield, Proc. Natl. Acad. Sci. **71**, 4135 (1974).
- [19] C. H. Bennett, Biosystems **11**, 85 (1979).
- [20] H. Qian, J. Mol. Biol. **362**, 387 (2006).
- [21] G. Lan, P. Sartori, S. Neumann, V. Sourjik, and Y. Tu, Nat. Phys. **8**, 422 (2012).
- [22] P. Mehta and D. J. Schwab, Proc. Natl. Acad. Sci. U. S. A. **109**, 17978 (2012).
- [23] A. Murugan, D. A. Huse, and S. Leibler, Proc. Natl. Acad. Sci. U. S. A. **109**, 12034 (2012).
- [24] A. C. Barato and U. Seifert, Phys. Rev. E **95**, 062409 (2017).
- [25] See Supplemental Material at <http://vaikuntanathan-group.uchicago.edu/SIupload>.
- [26] R. R. Aldrovandi, *Special matrices of mathematical physics : stochastic, circulant, and Bell matrices* (World Scientific, 2001) p. 323.
- [27] S. Vaikuntanathan, T. R. Gingrich, and P. L. Geissler, Phys. Rev. E. **89**, 1 (2014).
- [28] A. Crisanti, G. Paladin, and A. Vulpiani, *Products of random matrices in statistical physics* (Springer, 1993) p. 166.
- [29] A. Amir, N. Hatano, and D. R. Nelson, Phys. Rev. E **93**, 042310 (2016).
- [30] L. Onsager, Phys. Rev. **65**, 117 (1944).
- [31] R. A. Marcus, J. Phys. Chem. A **105**, 2612 (2001).
- [32] K. Terauchi, Y. Kitayama, T. Nishiwaki, K. Miwa, Y. Murayama, T. Oyama, and T. Kondo, Proc. Natl. Acad. Sci. U.S.A **104**, 16377 (2007).